JMEPEG (2005) 14:417-423
DOI: 10.1361/105994905X56115

1059-9495/$19.00

Nanoindentation Behavior of Nanolayered Metal-Ceramic Composites

X. Deng, C. Cleveland, T. Karcher, M. Koopman, N. Chawla, and K.K. Chawla

(Submitted April 27, 2005; in revised form May 12, 2005)

Small-length scale multilayered structures are attractive materials due to their extremely high strength and flexibility, relative to conventional laminated composites. In this study, nanolayered laminated composites of Al and SiC were synthesized by DC/RF magnetron sputtering. The microstructure of the multilayered structures was characterized, and the mechanical properties measured by nanoindentation testing. The influence of layer thickness on Young's modulus and hardness of individual and multilayers was quantified. An analytical model was used to subtract the contribution of the Si substrate, to extract the true modulus of the films.

Keywords Al-SiC composite, laminated composite, magnetron sputtering, nanoindentation, nanomaterials

1. Introduction

Nanomaterials are very promising materials that exhibit ultrahigh strength with decreasing grain size to the nanometer scale (Ref 1-3). In particular, the strength of single and multilayered films has been shown to be significantly higher than that of bulk materials. Single metallic films (Ref 4-11), multilayered metal films (Ref 10, 12, 13), metal-ceramic layered composites (Ref 14-25), and ceramic-ceramic layered composites (Ref 26, 27) were investigated. A wide variety of processing techniques were explored to synthesize single or multilayered films at the nanoscale. These include chemical vapor deposition (CVD), physical vapor deposition (PVD) (Ref 4-28), electroplating (Ref 29-31), and the sol-gel technique (Ref 32, 33). Compared with other processes, PVD has the advantage of simplicity, relatively low processing temperatures, and a wide range of materials that can be processed. The PVD process, particularly magnetron sputtering, has been used to synthesize thin films of several metals, alloys, and ceramics.

Among metal-ceramic multilayered films, Al/Al_2O_3 has been the most commonly studied system. It is typically processed by reactive magnetron sputtering method by introducing oxygen to form Al_2O_3 at predetermined intervals (Ref 14). A limitation of the reactive sputtering, in this case, is the thickness of Al_2O_3 is limited by the kinetics of oxidation of Al. Similar methods for introducing reaction gases during metal deposition have been used to produce ceramic reinforcement, e.g., TiN (Ref 15, 21, 23), CrC (Ref 19), and CrN (Ref 25). Direct sputtering of ceramic targets has not really been studied, although metal-ceramic films containing $MoSi_2$ (Ref 17) and Bi_2O_3 (Ref 28) have been reported.

In this paper, processing and mechanical behavior results are presented on a novel metal-ceramic system, Al-SiC. The combination of Al and SiC were exploited to obtain high strength and stiffness in conventional fiber reinforced (Ref 34), particle reinforced composites (Ref 35), and bulk laminates (Ref 36). This combination has not, however, been examined in multilayers at the nanoscale. In this study, multilayered Al-SiC composites, as well as single layers of Al and SiC, were synthesized by direct current (dc) radio frequency (rf) magnetron sputtering on Si (111) single-crystal wafers. Instrumented indentation was used to probe the properties of single and multilayered materials.

2. Experimental Procedure

A magnetron sputtering system (Fig. 1) was used to deposit the multilayered composite used in this study. Al and SiC layers were deposited on Si (111) single-crystal wafers by dc and rf power, respectively. Aluminum targets (>99.99% purity) were sputtered at a dc power of 95 watts and Ar working pressure of 3.0 mtorr. SiC layers were produced from a sintered target (>99.5% purity) using identical argon pressure and an rf power of 215 W. Prior to deposition, an average base pressure in the range of 1.3×10^{-5} Pa was obtained. Target presputtering was carried out to remove oxides or contaminants prior to film deposition. The substrate was also rotated during deposition to ensure a uniform nanolayer. Deposition rates for both materials were obtained by producing a graded composite film. The deposition time was continuously varied, starting with SiC and then alternating layers of Al and SiC. Individual layer thicknesses were then measured from several scanning electron microscopy (SEM) micrographs. Figure 2(a) illustrates the composite layers used in obtaining the deposition rates, and Fig. 2(b) shows the linear growth profiles for both Al and SiC.

This paper was presented at the International Symposium on Manufacturing, Properties, and Applications of Nanocrystalline Materials sponsored by the ASM International Nanotechnology Task Force and TMS Powder Materials Committee on October 18-20, 2004 in Columbus, OH.

X. Deng, C. Cleveland, and **N. Chawla,** Department of Chemical and Materials Engineering, Fulton School of Engineering, Arizona State University, Tempe, AZ 85287-6006; **T. Karcher,** Center for Solid State Science, College of Liberal Arts and Science, Arizona State University, Tempe, AZ 85287; and **M. Koopman** and **K.K. Chawla,** Department of Materials Science and Engineering, University of Alabama at Birmingham, Birmingham, AL 35209. Contact e-mail: Nikhilesh.Chawla@asu.edu.

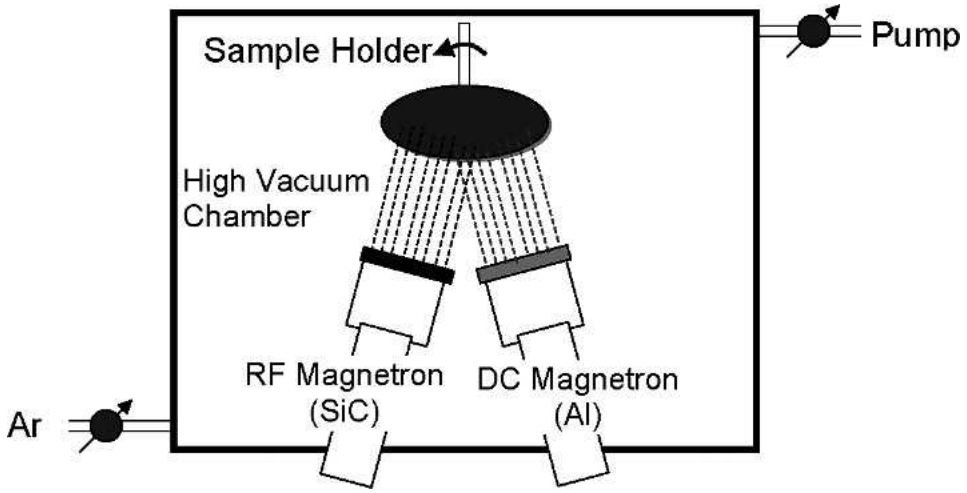

Fig. 1 Schematic illustration of the magnetron sputtering system used in this study

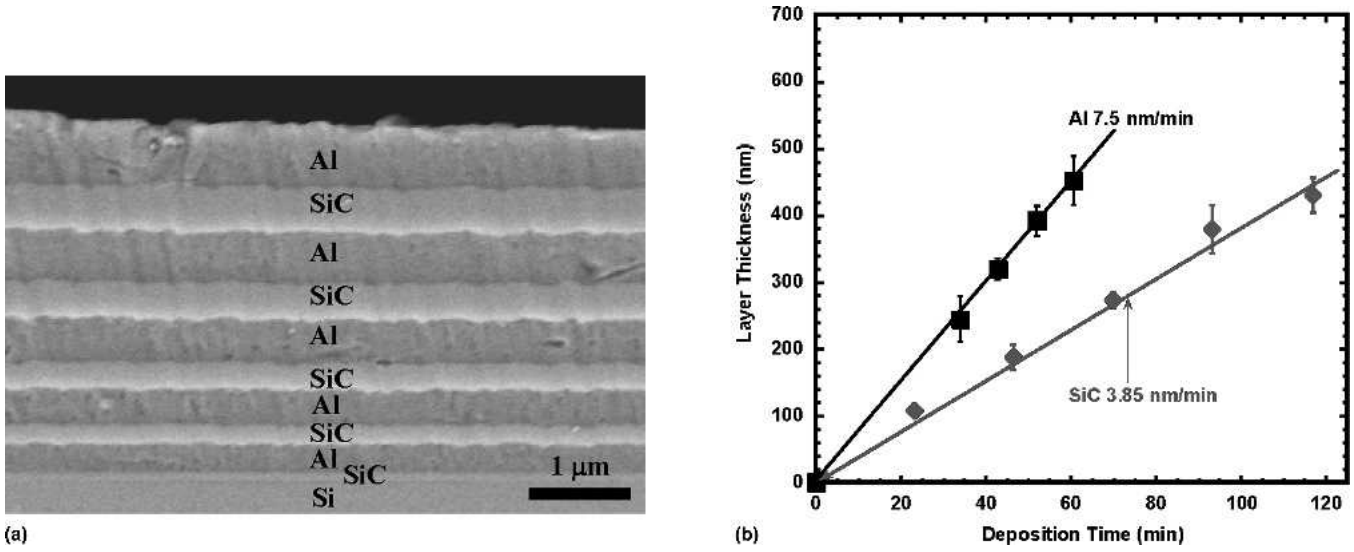

Fig. 2 (a) Al-SiC multilayer composite with different thickness of layer, and (b) layer thickness versus deposition time of Al and SiC. The extrapolated growth rate was used further for the fabrication of Al, SiC single layers, and Al-SiC multilayer.

Deposition rates of approximately 7.5 and 3.9 nm/min were obtained for Al and SiC, respectively.

Both multilayers of Al/SiC and single layers of Al and SiC were deposited on Si wafers based on the deposition rates obtained in Fig. 2(b). The thickness of the individual films was varied between 100 and 1000 nm. Multilayers of Al-SiC had seven total layers (three of SiC, each of 33 nm thickness, and four of Al, each of 100 nm thickness). Nanoindentation was carried out on both single-layered and mutilayered samples. Approximately 30 indentations were made for each film at a given thickness. Calibration of the indenter was conducted by measuring the Young's modulus and hardness of a silica standard. The continuous stiffness measurement (CSM) technique was used during indentation (Ref 37, 38). This technique involves the application of a harmonic, high frequency amplitude force during indentation loading, and measurement of the contact stiffness of the sample from the displacement response at the excitation frequency. The Young's modulus of the material is then derived from the contact stiffness. In all measurements, the Young's modulus and hardness were evaluated as a function of depth. As a result of the influence of the Si substrate, the Young's modulus of the multilayers was extracted from the experimental curves using the model by Gao et al. (Ref 39).

3. Results and Discussion

3.1 Indentation Behavior

The indentation behavior of single layers of Al and SiC is described first. Figure 3 shows the load-displacement curves for Al and SiC single layers with varying thickness. The influence of the Si (111) substrate is significant. For the Al layers, which are softer than the Si substrate, at a given indentation depth (e.g., 100 nm), the thinnest film exhibited the highest load. The reverse was true of the SiC layers, which are stiffer and harder than the Si substrate. The Young's modulus of the individual films as a function of indentation depth also showed some interesting trends (Fig. 4). During instrumented indentation of bulk materials or even relatively thick films, the modulus exhibits a "plateau" over the initial displacement range (Ref

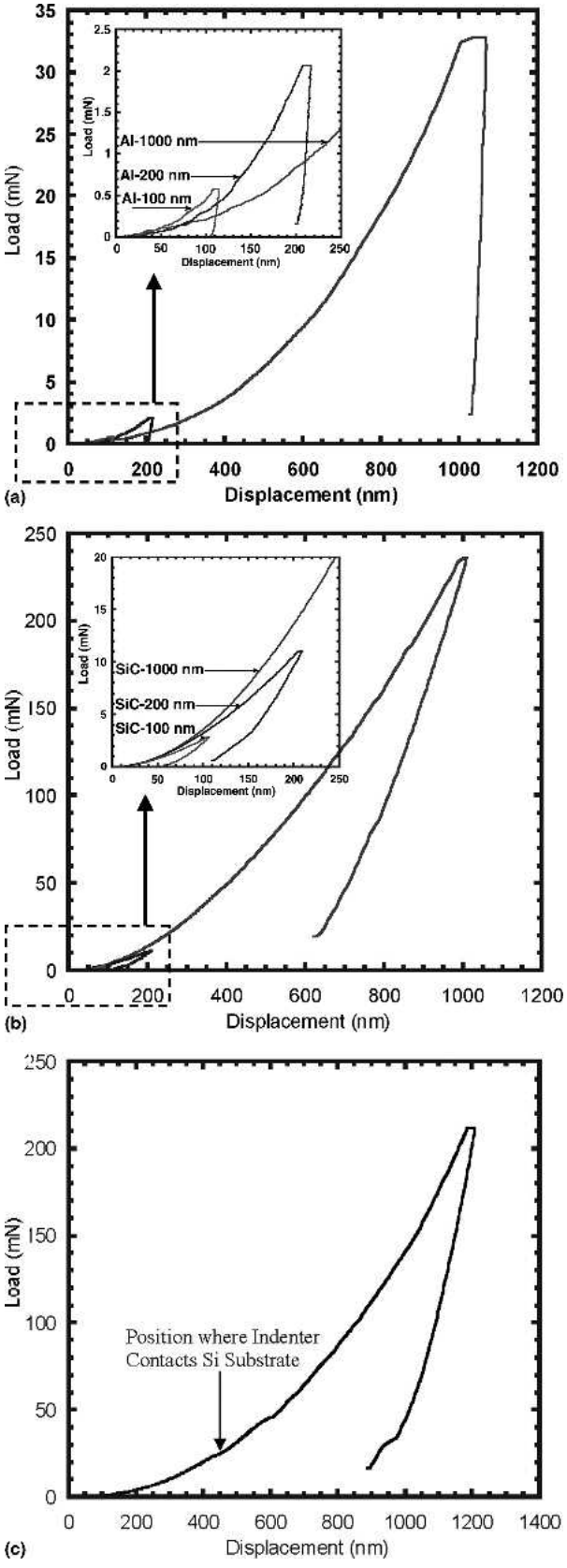

Fig. 3 Load-displacement curves for single layer of (a) Al, (b) SiC with different thickness, and multilayer of (c) Al-SiC. Layer thickness has a significant effect on the indentation behavior. The increased thickness of softer layer (compared with Si substrate) leads to the lower load-displacement behavior whereas for the harder layer, the trends are on the contrary.

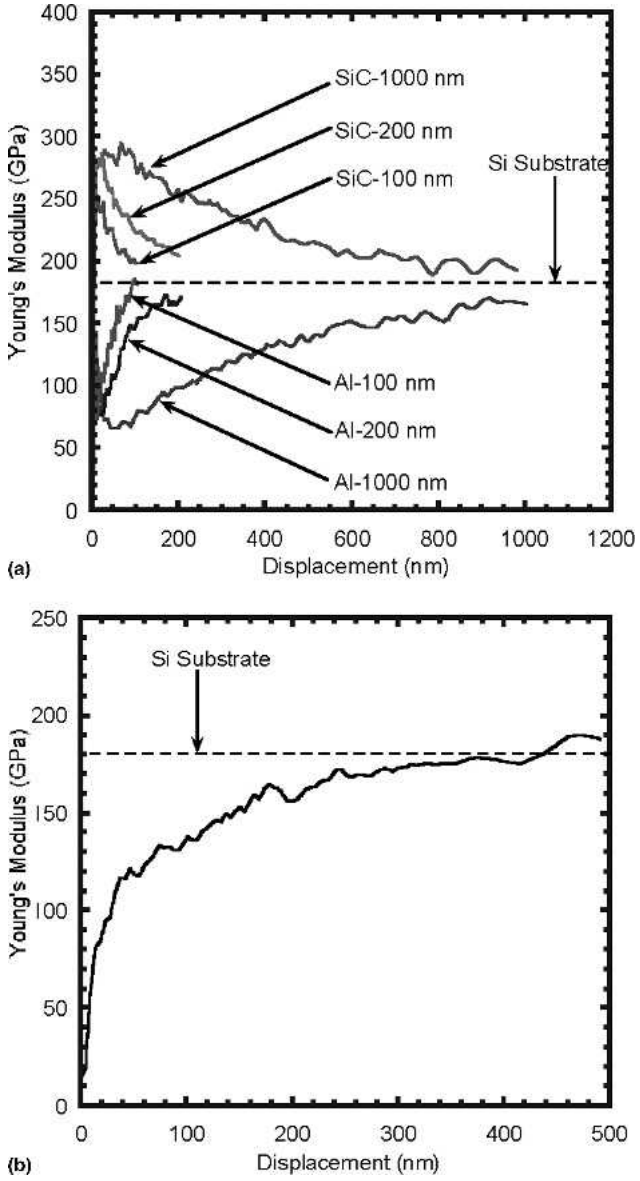

Fig. 4 Young's modulus of (a) SiC and Al single layers, and (b) Al-SiC multilayer as a function of indentation displacement. There is no considerable plateau due to the influence from Si (111) substrate, and Young's modulus of all layers tends to approach the value of Si substrate along with the displacement.

40, 41). In the films studied here, no visible stable region of constant modulus was observed. This is attributed to the relatively small thickness of the layers, which results in a significant contribution of the substrate to the indentation behavior. Consider that the Young's modulus of the Al layers, independent of thickness, increases continuously with the indentation depth and tends to approach the Young's modulus of the Si substrate. For the SiC layer, the modulus decreased continuously with indentation depth approaching the stiffness of the Si substrate. Several models have been proposed that account for the influence of substrate properties on the modulus of thin films (Ref 39, 42-47). In this paper, the relation proposed by Gao et al. (Ref 39) is used to extrapolate the Young's modulus of the film, E_f:

$$E - E_s = (E_f - E_s)\Phi_{Gao} \quad \text{(Eq 1)}$$

Table 1 Young's modulus and hardness of Al and SiC nanolayers and Al-SiC multilayer

Layer	Young's modulus, GPa	Hardness, GPa
Al (200 nm)	43 ± 13	1.06 ± 0.21
Al (1000 nm)	43 ± 12	0.68 ± 0.09
SiC (200 nm)	280 ± 14	25.7 ± 1.4
SiC (1000 nm)	281 ± 6	25.9 ± 0.9
Al-SiC multilayer	71 ± 17	2.4 ± 0.3

where E is the measured composite (layer + substrate) modulus, E_s is the modulus of the substrate, and Φ_{Gao} is a function that is expressed as:

$$\Phi_{Gao} = \frac{2}{\pi}\arctan\frac{1}{x} + \frac{1}{2\pi(1-\nu)}\left[(1-2\nu)\frac{1}{x}\ln(1+x^2) - \frac{x}{1+x^2}\right] \quad \text{(Eq 2)}$$

where $x = a/t$, a is the mean radius of the projected contact area, which is a linear function of indentation depth, t is the film layer thickness, and ν is the Poisson's ratio of film. E is measured experimentally, and E_s for Si (111) substrate is about 180 GPa (Ref 48). The calculated values of the Young's modulus of SiC and Al nanolayer are shown in Table 1. Young's modulus is independent of layer thickness for both Al and SiC. This indicates that the defect population in the film does not appear to be a function of film thickness. Young's modulus of both Al and SiC is significantly lower than that of their bulk counterparts (Ref 49). This can be attributed to intrinsic defects formed during processing, such as nanovoids (Ref 10). In addition, preliminary x-ray diffraction (XRD) measurements indicate that the Al films are highly textured (Ref 50), which is consistent with other research (Ref 51). Furthermore, XRD and preliminary transmission electron microscopy (TEM) work indicate that the SiC films are amorphous/nanocrystalline. The amorphous structure of SiC is likely caused by the low processing temperature used here. In this study, the processing temperature was less than 200 °C. Leiste et al. (Ref 52) produced SiC films by the rf sputtering method, and their XRD analysis shows that the SiC remains amorphous up to a processing temperature of 500 °C.

Hardness measurements were also obtained from indentation for both Al and SiC (Fig. 5). Due to the influence of the Si substrate, the measured hardness also varied significantly with indentation depth. The hardness of Al increased with indentation depth due to the higher pileup in the Al caused by the harder Si substrate (Ref 44). The hardness also increased with decreasing thickness of the Al layer. In the early stages of indentation, there was some scatter in the measured hardness, especially for thickness of 100 and 200 nm. The roughness of Al surface (Fig. 6), may have contributed to this scatter, as documented by Bouzakis et al. (Ref 53). The hardness of SiC decreased with indentation depth as a result of the early onset of yielding of the Si substrate (Ref 44). Both the 1000 nm Al and 1000 nm SiC exhibited a plateau in hardness between 100 and 200 nm of indentation depth. The pileup effect for the Al layers or the yielding of Si for SiC layers is not significant at this depth range, so the hardness value of Al and SiC nanolayer was calculated as the average in this range, as shown in Table 1. The hardness for Al and SiC of 200 nm thickness, taken between 20 and 40 nm, is also listed in Table 1 to show the effect of film thickness. Compared with Al at 1000 nm, the 200 nm thick layer had a much higher hardness. This is mainly due to the influence from the harder Si substrate. For SiC, the hardness varies very little with film thickness, because the influence of the Si substrate is not as significant.

The indentation load-displacement curve for Al-SiC multilayers is shown in Fig. 3(c). The Young's modulus versus depth plot (Fig. 4b), did not exhibit a stable plateau, perhaps due to the influence of the Si substrate, so the model from Gao et al. (Ref 39) was used to extrapolate the Young's modulus of multilayers of Al-SiC. The hardness-displacement curve, Fig. 5(c) does show a plateau between 50 and 100 nm. The hardness of multilayers of Al-SiC was extracted as the average of the hardness at this depth range. Table 1 shows that the magnitude of both Young's modulus and hardness of Al-SiC multilayer is between that of Al and SiC single layer. The indentation morphology of the Al-SiC multilayer is shown in Fig. 7. The indenter has completely penetrated the multilayer and gone into the Si substrate. Significant pileup is observed at the edge of indentation, mainly due to the plastic deformation of Al layer.

The Young's modulus of the Al-SiC multilayer E_c can be modeled by a simple rule-of-mixtures because the Al and SiC are in an isostrain condition. The Young's modulus of the Al layer, E_{Al}, and SiC layer, E_{SiC}, the volume fraction of Al, V_{Al}, and SiC layer, V_{SiC}, are known. The modulus is then given by:

$$E_c = E_{Al}V_{Al} + E_{SiC}V_{SiC} \quad \text{(Eq 3)}$$

Taking the data in Table 1 for E_{Al} (43 GPa), E_{SiC} (281 GPa), and V_{Al} 0.8, V_{SiC} 0.2 from the layer thickness, Eq 3 gives $E_c = 91$ GPa, which is somewhat higher than the experimental value of 71 GPa.

It is interesting to compare the mechanical properties of the single layers in this study with other studies, although direct comparisons to measurements from other researchers is often complicated by factors such as grain size, texture, defects, strain rate, and impurity content (Ref 6). Read et al. (Ref 6) deposited 1 μm thick Al layer on Si wafer by electron beam evaporation process. The free standing Al layer for testing was obtained by etching off the Si substrate. Young's modulus measurements, from tensile tests, varied between 24 and 30 GPa. Kang et al. (Ref 7) deposited 60-480 nm thick Al on Kapton by magnetron sputtering. They found a strong (111) texture in the Al film. The Young's modulus extrapolated from the tensile stress-strain curve was about 20.8 GPa. Haque and Saif (Ref 8) produced 30 and 50 nm thick freestanding Al by sputtering process. Their TEM observation did not show any pores or voids within the material. Their Young's modulus values, also measured in tension, were as high as 60 GPa. The values for Al films are in the range reported in the literature (~43 GPa). As mentioned above, this may be attributed to the presence of nanovoids. Young's modulus measurements of SiC films are scarce. The Vickers hardness of SiC studied by Leiste et al. (Ref 52) and Seo et al. (Ref 54), which appears to be the same for crystalline or amorphous structure, varied between 24 and 28 GPa. These hardness results are similar to the values reported here.

Very little work, if any, has been done on the mechanical behavior of Al-SiC nanolayers. Other investigated metal-ceramic nanolayer systems include Al-Al_2O_3 (Ref 14, 16) and Mo-Al_2O_3 (Ref 17). Mearini and Hoffman (Ref 16) produced pure Al, Al_2O_3, as well as Al-Al_2O_3 nanolayer by the PVD process. The Al_2O_3 layers had an amorphous structure and very low Young's modulus (107-110 GPa). The Young's modulus of Al-Al_2O_3 nanolayer (total thickness 182-328 nm, 30 layers

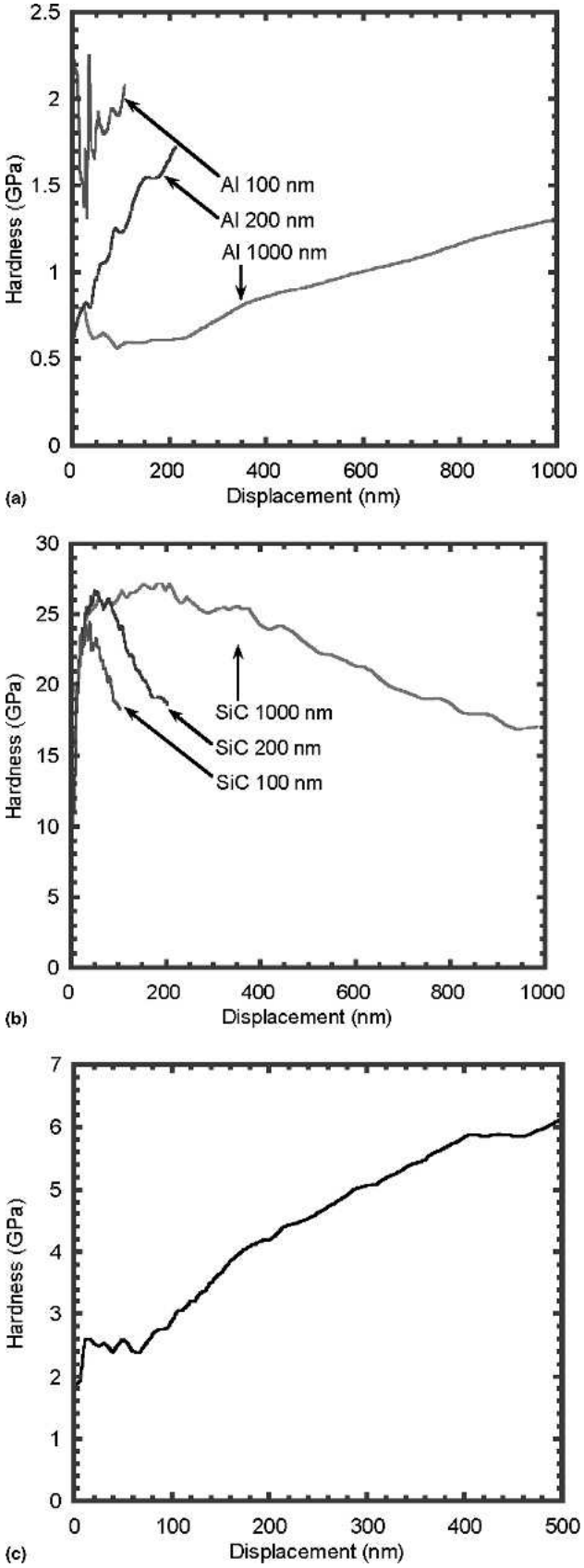

Fig. 5 Hardness versus indentation displacement for single layer of (a) aluminum and (b) SiC nanolayer with different thickness, and multilayer of (c) Al-SiC. A very short plateau shows up at the beginning of indentation. Thicker layers have more stable and longer plateau.

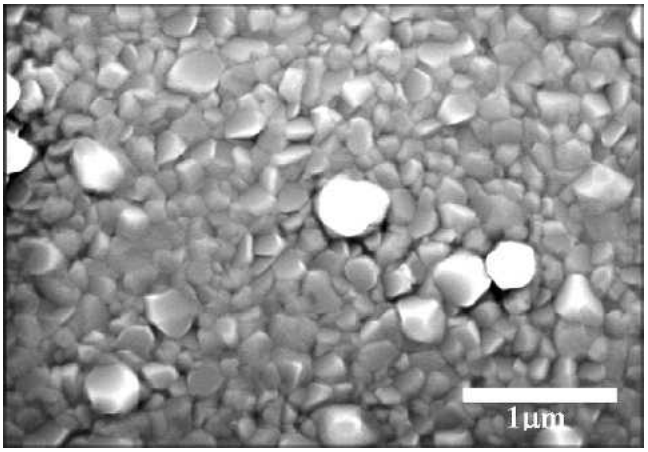

Fig. 6 Surface of Al nanolayer. The roughness of surface may contribute to the scatter in hardness at early stages of nanoindentation.

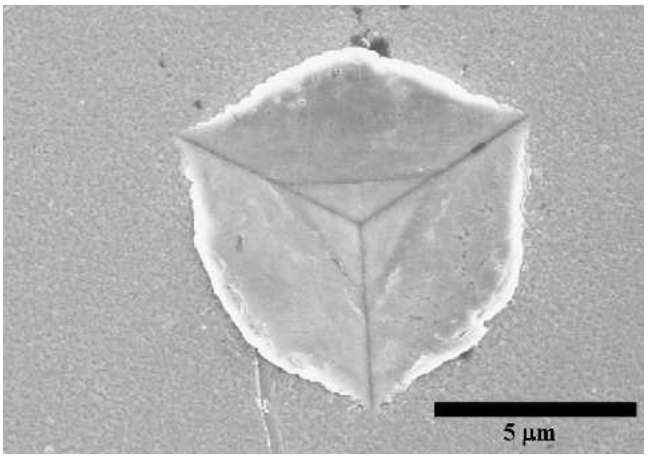

Fig. 7 Indentation morphology of Al-SiC multilayer. Significant pileup takes place at the edges of the indentation due to the plastic deformation of Al.

Al_2O_3, about 50 vol.% Al_2O_3) was 68 GPa and ultimate tensile strength (UTS) varied between 122 and 414 MPa. Alpas et al. (Ref 14) conducted tensile tests on Al/Al_2O_3 nanolayers with different Al layer thickness (Al_2O_3 layer thickness was less than 10 nm). The yield strength of 450 MPa was achieved when the Al layer thickness was 50 nm and the strength decreased to 180 MPa when the Al layer thickness increased to 500 nm. Chou et al. (Ref 17) fabricated Mo-Al_2O_3 nanolayers as well as Mo and Al_2O_3 monolithic layer on Si (111) by dc and rf reactive sputter deposition. TEM observation showed that Al_2O_3 was amorphous with some crystalline islands whereas Mo was polycrystalline. Nanoindentation tests showed that Young's modulus of Al_2O_3 was about 150 GPa and the hardness 9.5 GPa. Mo-Al_2O_3 nanolayer has 50 vol.% Al_2O_3 with different interlayer spacing (5-100 nm). 100 nm interlayer spacing yielded the highest Young's modulus (250 GPa) and hardness (16 GPa).

The Hall-Petch equation had an extremely high prediction of yield strength, which is typically not observed in nanostructured materials. It is possible that the intrinsic defects during processing resulted in a much lower strength than the Hall-Petch prediction. For nanolayered composite, interlayer spacing appears to be the most significant factor in determining the

strength. Koehler (Ref 55) and Lehoczky (Ref 56) gave a more effective strengthening mechanism compared with Hall-Petch relation for laminated composites. In Lehoczky's model, there is a critical value of interlayer spacing λc, the yield strength of nanolayered composite is proportional to λ^{-1} when $\lambda > \lambda c$. When $\lambda < \lambda c$, the yield strength remains constant or decreases. Further investigation of the effect of Al-SiC nanolayer thickness is important.

4. Conclusions

The following conclusions can be made from this study of the nanoindentation behavior of Al, SiC, and Al-SiC multilayers on the nanoscale:

- Al, SiC, and Al/SiC nanolayered composites were synthesized by dc/rf magnetron sputtering process.
- Nanoindentation showed that the Young's modulus of Al and SiC nanolayer were lower than that of bulk materials. The presence of defects may have contributed to the lower elastic modulus.
- Multilayered Al/SiC exhibited much higher Young's modulus and hardness than the pure Al layer.

References

1. A.M. El-Sherik, U. Erb, G. Palumbo, and K.T. Aust, Deviations from Hall-Petch Behaviour in As-Prepared Nanocrystalline Nickel, *Scr. Metall. Mater.,* Vol 27 (No. 9), 1992, p 1185-1188
2. Y. Wang and N. Herron, Nanometer-Sized Semiconductor Clusters: Materials Synthesis, Quantum Size Effects, and Photophysical Properties, *J. Phys. Chem.,* Vol 95 (No. 2), 1991, p 525-532
3. S. Zhang, D. Sun, Y. Fu, and H. Du, Recent Advances of Superhard Nanocomposite Coatings: A Review, *Surf. Coat Technol.,* Vol 167, 2003, p 113-119
4. D.T. Read, Tension-Tension Fatigue of Copper Thin Films, *Int. J. Fatigue,* Vol 20, 1998, p 203-209
5. Y.W. Yu Denis and Frans Spaepen, The Yield Strength of Thin Copper Films on Kapton, *J. Appl. Phys.,* Vol 95, 2004, p 2991-2997
6. D.T. Read, Yi-Wen Cheng, R.R. Keller, and J.D. McColskey, Tensile Properties of Free-Standing Aluminum Thin Films, *Scr. Mater.,* Vol 45, 2001, p 583-589
7. Y.S. Kang and P.S. Ho, Thickness Dependent Mechanical Behavior of Submicron Aluminum Films, *J. Electron. Mater.* 1997, Vol 26 (No. 7), 1997, p 805-813
8. M.A. Haque and M.T. Saif, Mechanical Behavior of 30-50 nm Thick Aluminum Films Under Uniaxial Tension, *Scr. Mater.,* Vol 47, 2002, p 863-867
9. F.R. Brotzen, Mechanical Testing of Thin Films, *International Materials Reviews,* Vol 39 (No. 1), 1994, p 24-45
10. H. Huang and F. Spaepen, Tensile Testing of Free-Standing Cu, Ag, and Al Thin Films and Ag/Cu Multilayers, *Acta Mater.,* Vol 48, 2000, p 3261-3269
11. D.T. Read and J.W. Dally, Fatigue of Microlithographically-Patterned Free-Standing Aluminum Thin Film Under Axial Stresses, *J. Electron. Packaging,* Vol 117, 1995, p 1-6
12. C. Daniel, A. Lasagni, and F. Mucklich, Stress and Texture Evolution of Ni/Al Multi-Film by Laser Interference Irradiation, *Surf. Coat Technol.,* Vol 180-181, 2004, p 478-482
13. J. Schumann, W. Brückner, and A. Heinrich, Properties and Applications of Vacuum-Deposited Cu-Cr Films, *Thin Solid Films,* Vol 228, 1993, p 44-48
14. A.T. Alpas, J.D. Embury, D.A. Hardwick, and R.W. Springer, The Mechanical Properties of Laminated Microscale Composites of Al/Al_2O_3, *J. Mater. Sci.,* 1990, Vol 25, 1990, p 1603-1609
15. D.O. Northwood and A.T. Alpas, Mechanical and Tribological Properties of Nanocrystalline and Nanolaminated Surface Coatings, *Nanostruct. Mater.,* 1998, Vol 10 (No. 5), 1998, p 777-793
16. G.T. Mearini and R.W. Hoffman, Tensile Properties of Aluminum/Alumina Multi-Layered Thin Films, *J. Elect. Mater.,* Vol 22 (No. 6), 1993, p 623-629
17. T.C. Chou, T.G. Nieh, S.D. McAdams, G.M. Pharr, and W.C. Oliver, Mechanical Properties and Microstructures of Metal/Ceramic Microlaminates: Part II. A Mo/Al_2O_3 System, *J. Mater. Res.,* Vol 7 (No. 10), 1992, p 2774-2784
18. C.H. Liu, Wen-Zhi Li, and Heng-De Li, TiC/Metal Nacreous Structures and Their Fracture Toughness Increase, *J. Mater. Res.,* Vol 11 (No. 9), 1996, p 2231-2235
19. J. Romero, A. Lousa, E. Martinez, and J. Esteve, Nanometric Chromium/Chromium Carbide Multilayers for Tribological Applications, *Surf. Coat. Technol.,* Vol 163-164, 2003, p 392-397
20. T.C. Chou, T.G. Niwh, T.Y. Tsui, G.M. Pharr, and W.C. Oliver, Mechanical Properties and Microstructures of Metal/Ceramic Microlaminates: Part I. Nb/MoSi2 Systems, *J. Mater. Res.,* Vol 7 (No. 10), 1992, p 2765-2773
21. M. Ben Daia, P. Aubert, S. Labdi, C. Sant, F.A. Sadi, Ph. Houdy, and J.L. Bozet, Nanoindentation Investigation of Ti/TiN Multilayers Films, *J. Appl. Phys.,* Vol 87, 2000, p 7753-7757
22. Jeong Hoon Lee, Won Mok Kim, Taek Sung Lee, Moon Kyo Chung, Byung-ki Cheong, and Soon Gwang Kim, Mechanical and Adhesion Properties of Al/AlN Multilayered Thin Films, *Surf. Coat. Technol.,* Vol 133-134, 2000, p 220-226
23. T. de los Arcos, P. Oelhafen, U. Aebi, A. Hefti, M. Duggelin, D. Mathys, and R. Guggenheim, Preparation and Characterization of TiN-Ag Nanocomposite Films, *Vacuum,* Vol 67, 2002, p 463-470
24. M.A. Phillips, B.M. Clemens, and W.D. Nix, Microstructure and Nanoindentation Hardness of Al/Al_3Sc Multilayers, *Acta Mater.,* Vol 51, 2003, p 3171-3184
25. A. Lousa, J. Romero, E. Martýnez, J. Esteve, F. Montala, and L. Carreras, Multilayered Chromium/Chromium Nitride Coatings for Use in Pressure Die-Casting, *Surf. Coat. Technol.,* Vol 146-147, 2001, p 268-273
26. D-H. Kuo and K-H. Tzeng, Characterization and Properties of R.F.-Sputtered Thin Films of the Alumina-Titania System, *Thin Solid Films,* Vol 460, 2004, p 327-334
27. V.P. Godbole, K. Dovidenko, A.K. Sharma, and J. Narayan, Thermal Reactions and Micro-Structure of TiN-AlN Layered Nano-Composites, *Mater. Sci. Eng.,* Vol B68, 1999, p 85-90
28. P. Zhou, H-Y. You, J-H. Jia, J. Li, T. Han, S-Y. Wang, R-J. Zhang, Y-X. Zheng, and L-Y. Chen, Concentration and Size Dependence of Optical Properties of Ag:Bi_2O_3 Composite Films by Using the Co-Sputtering Method, *Thin Solid Films,* Vol 455-456, 2004, p 605-608
29. B. Miller and H. Ferkel, $A1_2O_3$-Nanoparticle Distribution in Plated Nickel Composite Films, *Nanostruct. Mater.,* Vol 10 (No. 8), 1998, p 1285-1288
30. A. Robertson, U. Erb, and G. Palumbo, Practical Applications for Electrodeposited Nanocrystalline Materials, *Nanostruct. Mater.,* Vol 12, 1999, p 1035-1040
31. A. Moller and H. Hahn, Synthesis and Characterization of Nanocrystalline Ni/ZrO2 Composite Coatings, *Nanostruct. Mater.,* Vol 12, 1999, p 259-262
32. D. Sporn. J. Großmann. A. Kaiser. R. Jahn, and A. Berger, Sol-Gel Processing of Nanostructured Ceramic and Ceramic/Metal Composite Materials, *Nanostruct. Mater.,* Vol 6, 1995, p 329-332
33. W. Liu, Y. Chen, G. Kou, T. Xu, and D.C. Sun, Characterization and Mechanical/Tribological Properties of Nano Au-TiO_2 Composite Thin Films Prepared by a Sol-Gel Process, *Wear,* Vol 254, 2003, p 994-1000
34. A. Colclough, B. Dempster, Y. Favry, and D. Valentin, Thermomechanical Behaviour of SiC-A1 Composites, *Mater. Sci. Eng. A,* Vol 135, 1991, p 203-207
35. V. Ganesh and N. Chawla, Effect of Reinforcement-Particle-Orientation Anisotropy on the Tensile and Fatigue Behavior of Metal-Matrix Composites, *Metall. Mater. Trans. A,* Vol 35A, 2004, p 53-61
36. C.K. Syn, D.R. Lesuer, and O.D. Sherby, Enhancing Tensile Ductility of a Particulate-Reinforced Aluminum Metal Matrix Composite by Lamination with Mg-9%Li Alloy, *Mater. Sci. Eng. A,* Vol 206, 1996, p 201-207
37. W.C. Oliver and G.M. Pharr, An Improved Technique for Determining Hardness and Elastic Modulus Using Load and Displacement Sensing Indentation Experiments, *J. Mater. Res.,* Vol 7 (No. 6), 1992, p 1564-1583
38. X. Li and B. Bhushan, A Review of Nanoindentation Continuous Stiffness Measurement Technique and Its Applications, *Mater. Characterization,* Vol 48, 2002, p 11-36
39. H. Gao, C. H. Chiu, and J. Lee, *Int. J. Solids Struct.,* Vol 29, 1992, p 2471-2492

40. X. Deng, N. Chawla, K.K. Chawla, and M. Koopman, *Acta Mater.,* Vol 52, 2004, p 4291-4303
41. X. Deng, M. Koopman, N. Chawla, and K.K. Chawla: *Mater. Sci. Eng.,* Vol 364, 2004, p 241-243
42. J. Mencik, D. Munz, E. Quandt, E.R. Weppelmann, and M.V. Swain, Determination of Elastic Modulus of Thin Layers Using Nanoindentation, *J. Mater. Res.,* Vol 12 (No. 9), 1997, p 2475-2484
43. M.F. Doerner and W.D. Nix, A Method for Interpreting the Data from Depth-Sensing Indentation Instruments, *J. Mater. Res.,* Vol 1, 1986, p 601-609
44. R. Saha and W.D. Nix, Effects of the Substrate on the Determination of Thin Film Mechanical Properties by Nanoindentation, *Acta Mater.,* Vol 50, 2002, p 23-38
45. R.B. King, Elastic Analysis of Some Punch Problems for a Layered Medium, *Int. J. Solids Struct.,* Vol 23, 1987, p 1657-1664
46. G.M. Pharr and W.C. Oliver, Measurement of Thin Film Mechanical Properties Using Nanoindentation, *MRS Bull.,* Vol 17 (No. 7), 1992, p 28-33
47. C. Gamonpilas and E.P. Busso, On the Effect of Substrate Properties on the Indentation Behaviour of Coated Systems, *Mater. Sci. Eng. A,* Vol 380, 2004, p 52-61
48. M.T. Kim, Influence of Substrates on the Elastic Reaction of Films for the Microindentation Tests, *Thin Solid Films,* Vol 283, 1996, p 12-16
49. N. Chawla,V.V.Ganesh, and B.Wunsch, Three-Dimensional (3D) Microstructure Visualization and Nite Element Modeling of the Mechanical Behavior of SiC Particle Reinforced Aluminum Composites, *Scr. Mater.,* Vol 51, 2004, p 161-165
50. X. Deng, unpublished data
51. Y.S. Kang and P.S. Ho, Thickness Dependent Mechanical Behavior of Submicron Aluminum Films, *J. Electron. Mater.,* Vol 26 (No. 7), 1997, p 805-813
52. H. Leiste, U. Dambacher, S. Ulrich, and H. Holleck, Microstructure and Properties of Multilayer Coatings with Covalent Bonded Hard Materials, *Surf. Coatings Technol.,* Vol 116-119, 1999, p 313-320
53. K-D. Bouzakis, N. Michailidis, S. Hadjiyiannis, G. Skordaris, and G. Erkens, The Effect of Specimen Roughness and Indenter Tip Geometry on the Determination Accuracy of Thin Hard Coatings Stress-Strain Laws by Nanoindentation, *Mater. Characterization,* Vol 49, 2003, p 149-156
54. J-Y. Seo, S-Y. Yoon, K. Niihara, and K.H. Kim, Growth and Microhardness of SiC Films by Plasma-Enhanced Chemical Vapor Deposition, *Thin Solid Films,* Vol 406, 2002, p 138-144
55. J.S. Koehler, Attempt to Design a Strong Solid, *Phys. Rev.,* Vol B2, 1970, p 547-551
56. S.L. Lehoczky, Retardation of Dislocation Generation and Motion in Thin-Layered Metal Laminates, *Phys. Rev. Lett.,* Vol 41, 1978, p 1814-1818